International Journal of Production Research

ISSN: 0020-7543 (Print) 1366-588X (Online) Journal homepage: http://www.tandfonline.com/loi/tprs20

One-dimensional-based automatic defect inspection of multiple patterned TFT-LCD panels using Fourier image reconstruction

D.-M. Tsai , S.-T. Chuang & Y.-H. Tseng

To cite this article: D.-M. Tsai , S.-T. Chuang & Y.-H. Tseng (2007) One-dimensional-based automatic defect inspection of multiple patterned TFT-LCD panels using Fourier image reconstruction, International Journal of Production Research, 45:6, 1297-1321, DOI: 10.1080/00207540600622464

To link to this article: https://doi.org/10.1080/00207540600622464

International Journal of Production Research,
Vol. 45, No. 6, 15 March 2007, 1297–1321

Taylor & Francis
Taylor & Francis Group

One-dimensional-based automatic defect inspection of multiple patterned TFT-LCD panels using Fourier image reconstruction

D.-M. TSAI*, S.-T. CHUANG and Y.-H. TSENG

Department of Industrial Engineering & Management, Yuan-Ze University, 135 Yuan-Tung Road, Nei-Li, Tao-Yuan, Taiwan, R.O.C

(*Revision received November 2005*)

Thin film transistor-liquid crystal display (TFT-LCD) has been used in a wide range of electronic devices. For large-sized and high-density TFT-LCD panel inspection, a high-resolution line scan is demanded. A TFT-LCD panel image at a fine resolution presents very complicated patterns with less regularity. The paper proposes a non-referential defect detection scheme that directly works on the one-dimensional (1D) line images using the Fourier image reconstruction. The 1D grey-level line image is first divided into small segments, each of the length of the repeated period for a given TFT-LCD panel. The divided segments are then combined as a two-dimensional (2D) image. The frequency components corresponding to the 1D background pattern can be easily identified in the 2D Fourier spectrum. By eliminating the frequency components in the 2D Fourier spectrum that represent the periodic structural pattern of the combined 2D image and then back-transforming the image using the inverse Fourier transform, the 2D Fourier reconstruction process can effectively remove the complicated background pattern and well preserve local anomalies. Experimental results on a number of micro-defects embedded in different patterned regions of TFT-LCD panels show that the proposed method can reliably detect various ill-defined defects.

Keywords: Automated inspection; Computer vision; Defect detection; Thin film transistor-liquid crystal display (TFT-LCD); Fourier transforms

1. Introduction

Flat panel displays are used in a wide range of electronic devices such as cellular phones, PDAs, computer monitors and television sets. Thin film transistor-liquid crystal display (TFT-LCD) has become a major technology for flat panel display in recent years due to its full-colour display capabilities, low power consumption and light weight. To ensure display quality and improve the yield of LCD flat panels, the inspection of defects in TFT-LCD panels becomes a critical task in LCD manufacturing.

In the LCD manufacturing process, perpendicular data and gate-conductive lines are patterned onto the glass substrate. A TFT-LCD panel comprises horizontal gate lines on one plane, and vertical data lines on the other plane. A thin film

*Corresponding author. Email: iedmtsai@saturn.yzu.edu.tw

International Journal of Production Research
ISSN 0020–7543 print/ISSN 1366–588X online © 2007 Taylor & Francis
http://www.tandf.co.uk/journals
DOI: 10.1080/00207540600622464

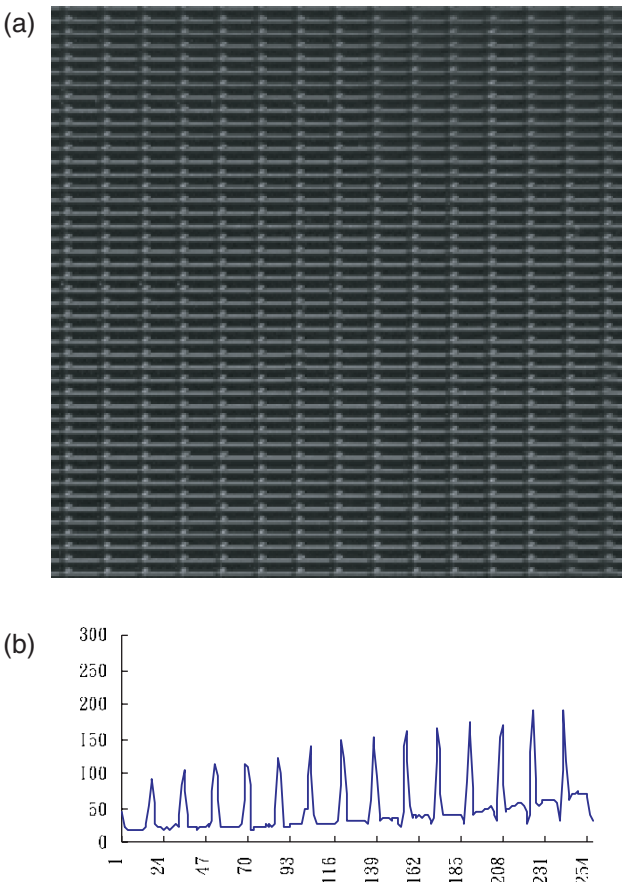

Figure 1. (a) Surface image of a TN-type TFT-LCD panel at a resolution of 60 pixels/mm; (b) a horizontal grey-level profile of the TFT-LCD image in (a).

transistor is located at each intersection of the data and gate lines (Pratt and Hawthorne 1998). The geometric structure of a TFT-LCD panel surface at a coarse resolution 60 pixels/mm, as shown in figure 1(a), involves repetitive, equally spaced horizontal and vertical lines. The TFT-LCD image under such a resolution can be therefore classified as a structural texture image that consists of an arrangement primarily of horizontal and vertical lines appearing periodically on the surface.

The surface defects of a TFT-LCD panel cause not only visual failure, but also electrical failure to operate the panel. There are currently several electrical and optical-based inspection techniques available for TFT-LCD defect inspection (Kido 1992, Chen *et al*. 2000, Hawthorne 2000, Lin *et al*. 2001). Henly and Addiego (1991) used an electro-optic modulator to generate voltage images. The voltage-imaging technique measures the characteristics of a TFT-LCD array by directly measuring the actual voltage distribution on the TFT pixel and not at the storage capacitor. Kido (1993) and Kido *et al*. (1995) presented an optical charge sensing technique for the inspection of active-matrix LCD panels. Charge sensing writes a charge to the

storage capacitor at the individual TFT array pixel. The charge is read back and compared with the write charge to determine if the pixel is defective (Hawthorne 2000). The advantage of the optical charge and voltage imaging approaches is that each pixel on the TFT panel can be individually tested. The main disadvantage of such approaches is that the probes used for voltage measurement must be separately designed for each panel configuration. With the fast development of LCD technologies, the new-generation polysilicon TFT-LCD displays with integrated drivers (Nakamura *et al*. 2002, Nishibe 2002) do not need storage capacitors. The charge-sensing and voltage-imaging methods will become useless since they cannot test arrays without storage capacitors.

A few vision-based techniques were developed for LCD defect inspection. The processing algorithm is typically either a computationally intensive pattern-matching, or a more straightforward image difference method (Hawthorne 2000). Nakashima (1994) presented an inspection system based on image subtraction and optical Fourier filtering for detecting defects in an LCD colour filter panel. The image subtraction method was employed to detect white and black defects such as black matrix holes and particles, and the optical Fourier filtering was applied for grain defects. Sokolov and Treskunov (1992) developed an automated visual system for final inspection of LCDs. They compared brightness distributions between a reference LCD image and a test image to detect anomalies in the surface. Maeda *et al*. (1999) proposed a template-matching-based system for detecting short-circuit defects in TFT substrates. The inspection image is obtained from a radiated infrared image that senses the heat of the short-circuit point by the leak current. The existing vision-based techniques generally need a prestored reference image for comparison. This requires large data storage for the reference image and precise environmental controls such as alignment and lighting for the TFT-LCD panel under inspection.

Oh *et al*. (2004) studied the detection of line-type defects in TFT-LCD panels. In a low-resolution image, a directional filter bank (DFB) that finds directional information is used to identify horizontal or vertical line-shaped defects. In a high-resolution image, a multilevel thresholding technique based on a statistical approach is employed to detect abnormal line defects that are brighter or darker than the surrounding pixels. Their approach is only applicable to line-shaped defects. Zhang and Zhang (2005) presented a fuzzy expert system to detect point defects, line defects and region defects in TFT-LCD panels. The defects are measured by the features of intensity contrast, area, location, direction and shape. The choice of proper defect features and design of fuzzy rules are time consuming, and highly rely on different types and characteristics of defects in question. Their proposed method can only detect defects in a coarse resolution image that contains only a uniform or a simple structural texture in the TFT-LCD panel surface.

Most of the vision-based techniques mentioned above are based on the analysis of grey levels in two-dimensional (2D) area images. Since there is an ongoing strong demand for the TFT-LCD used in large-screen computer monitors and televisions, large-sized TFT-LCD panel manufacturing is getting important. A high-resolution line scan, therefore, will be demanded for the inspection of large-sized TFT-LCD panels. Tsai and Hung (2005) proposed a one-dimensional (1D) Fourier-based image reconstruction scheme that directly works on the 1D line images instead of the

traditional 2D area images. Their method mainly focused on the twisted nematic (TN) TFT-LCD image at a coarse resolution such as that shown in figure 1(a), which comprises equally spaced horizontal and vertical lines. Figure 1(b) shows the grey-level profile of one horizontal scan line in figure 1(a). Each periodic peak in the profile represents a data line in the TFT-LCD surface. The distance between two adjacent peaks corresponds to the spacing between two neighbouring data lines. Any scan lines in such an image surface have similar periodic patterns as that shown in figure 1(b). Their method first eliminates the frequency components that represent the periodic peak pattern of the 1D grey level profile of a TFT-LCD line image in the 1D Fourier spectrum and then back-transforms the 1D Fourier-domain image using the 1D inverse Fourier transform. The Fourier reconstruction process can effectively remove the regularly patterned background and distinctly preserve local anomalies in the resulting 1D image. For a faultless TFT-LCD line image, the reconstruction process will result in a flat horizontal line. High fluctuation of a line will be generated in the reconstruction for a defective TFT-LCD line image.

For high-end display applications, recent developments in TFT-LCD have shifted from TN LCDs to multidomain vertical alignment (MVA) LCDs (Koike and Okamoto 1999, Park *et al*. 2003). MVA TFT-LCDs are based on the vertical alignment technique. They offer a wide viewing angle, a high contrast ratio and a fast response time. The geometric structure of an MVA TFT-LCD panel image is far more complicated than the TN TFT-LCD panel described previously. In addition, as the configuration of a TFT-LCD panel becomes dense, the fatal defects that generally have diameters around 20 μm can only be detected at a very high-resolution image, e.g. 500 pixels/mm. At such a high resolution, the sensed TFT-LCD image shows no simple homogeneous texture pattern. Figure 2(a) illustrates an MVA TFT-LCD panel image at a fine resolution of 500 pixels/mm. The MVA TFT-LCD panel surface not only involves horizontal gate line and vertical data lines, but also contains complicated patterns of common lines and TFTs. All these small, complicated patterns appear repetitively on the panel surface. Figure 2(b) demonstrates the grey-level profile of one horizontal scan line across the common-line region in figure 2(a). Periodicity feature is also presented in the grey-level profile. However, the pattern in each period is more complicated than the one in figure 1(b) that shows only one peak in each period. The 1D image reconstruction scheme proposed by Tsai and Hung (2005) cannot be directly extended to micro-defect detection in TFT-LCD panels at high image resolutions. The frequency components associated with the periodic background pattern of a TFT-LCD line image at a high resolution is not identifiable and cannot be removed from the corresponding 1D Fourier spectrum.

The present study also proposes a global Fourier reconstruction scheme to detect local anomalies in 1D line images of a TFT-LCD panel surface that involves various complicated patterns in different line images. Instead of directly reconstructing the 1D scan line using the 1D Fourier transforms, the less-regular grey-level profile in question is first divided into small segments, each of the length of the repeated period for a given TFT-LCD panel. The divided 1D segments are then combined as a 2D image. The periodicity feature of a 1D grey-level profile is much enhanced in the

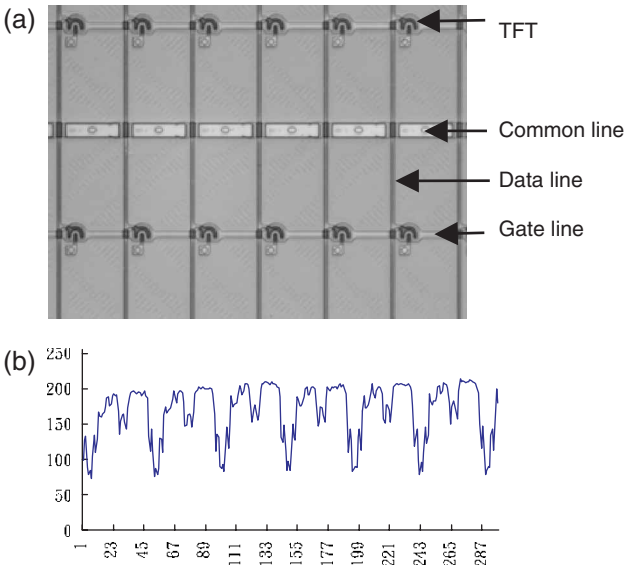

Figure 2. (a) Surface image of an MVA-type TFT-LCD panel at a high resolution of 500 pixels/mm; (b) a horizontal grey-level profile of the TFT-LCD image in (a).

combined 2D image and, therefore, the frequency components associated with the repetitive background pattern in the combined 2D image can be easily identified in the corresponding 2D Fourier spectrum. By eliminating the frequency components that represent the periodic structural pattern of the combined 2D image, and back-transforming the image using the 2D inverse Fourier transform, it will effectively remove the repetitive background pattern and well preserve local anomalies in the reconstructed image. The simple statistical control limits can then be used to set up the thresholds for distinguishing between anomalies and uniform background in individual reconstructed line images. This converts the difficult defect detection in a complexly patterned TFT-LCD panel image into a simple thresholding in a uniform image. The proposed method does not rely on the design of quantitative features to describe various defect types, nor does it require a template image for comparison. It alleviates all limitations of the feature extraction and template matching methods.

The paper is organized as follows. Section 2 describes the geometric structure of a TFT-LCD panel surface in the high-resolution image. The partition process that divides a 1D scanned line image into small segments of equal lengths is discussed, followed by the combination of the divided segments into a 2D image. 1D and 2D Fourier transforms, and the properties of a patterned TFT-LCD image in the Fourier spectrum are then described in detail. The removal of the repetitive background pattern of any 1D scanned line image in the combined 2D image is finally analysed. Section 3 presents the experimental results from a number of TFT-LCD test samples that contain various micro-defects embedded in different patterned regions of the TFT-LCD surfaces. Section 4 has conclusions.

2. Fourier reconstruction for patterned TFT-LCD line images

2.1 *Geometric structure of TFT-LCD panels at a high resolution*

As demonstrated in figure 2(a), a TFT-LCD panel surface image at the high resolution of 500 pixels/mm comprises vertical data lines, horizontal gate lines, common lines and TFTs. All these components repeatedly appeared in the panel surface. The resulting image can no longer be treated as a homogeneous structure texture due to the complicated patterns of common lines and TFTs. Note that the vertical data lines are equally spaced in the panel surface. The distance between two adjacent data lines thus gives the period of a fixed length for the TFT-LCD panel at a given resolution. The pattern between two adjacent data lines is repeated in the panel surface. For any horizontal scanned line image of a TFT-LCD panel surface, the patterns of one period in a line image should resemble each other, regardless of the position of the scan line across TFTs, common lines or data lines.

Figures 3(a1–c1) show three 2D images that contain particle defects in the pixel area, common-line region and TFT region, respectively. The line images in figures 3(a2–c2) are samples of horizontal grey-level profiles across the respective faultless regions in figures 3(a1–c1). Resembled patterns with the length of one period are repeated in every faultless line image. Note that the grey-level profile in the pixel area has the most simple and regular pattern, as shown in figure 3(a2). Visible periodic peaks are observed in the profile, in which each peak represents a data line. The patterns in the common-line and TFT regions are much more complicated and less stationary due to high grey-level variations of common lines and TFTs in the image. However, resemblance of the pattern in one period is still well preserved. Figures 3(a3–c3) are the scanned lines that crossover the particle defects in respective regions. The pattern associated with the particle defect in one periodic length is different to some extent from the normal one. The proposed method full uses the inherent characteristics of a TFT-LCD panel that it presents a periodic pattern in every scan line, and the length of the period is the same for all scan lines of the panel surface. Since a TFT-LCD panel at a high resolution involves various complicated patterns in different scan lines, the task in this study is then the detection of defects in multiple patterned surface images.

2.2 *Fourier image reconstruction*

The present study uses machine vision to tackle the problem of detecting micro-defects embedded in TFT-LCD panel surfaces with complicated patterns in high-resolution images. The line images, instead of the area images, of a TFT-LCD panel are used directly as the input for inspection in the manufacture of LCDs. Any scanned line image of a TFT-LCD panel surface shows a periodic grey-level profile. The Fourier transform has the desirable properties of noise-immunity, orientation preserving and enhancement of periodic features. With careful construction of the 1D line image, the Fourier spectrum is ideally suited for describing the periodicity of the patterned TFT-LCD panel surface. The global, periodic pattern can be distinguishable as concentration of high-energy bursts in the spectrum.

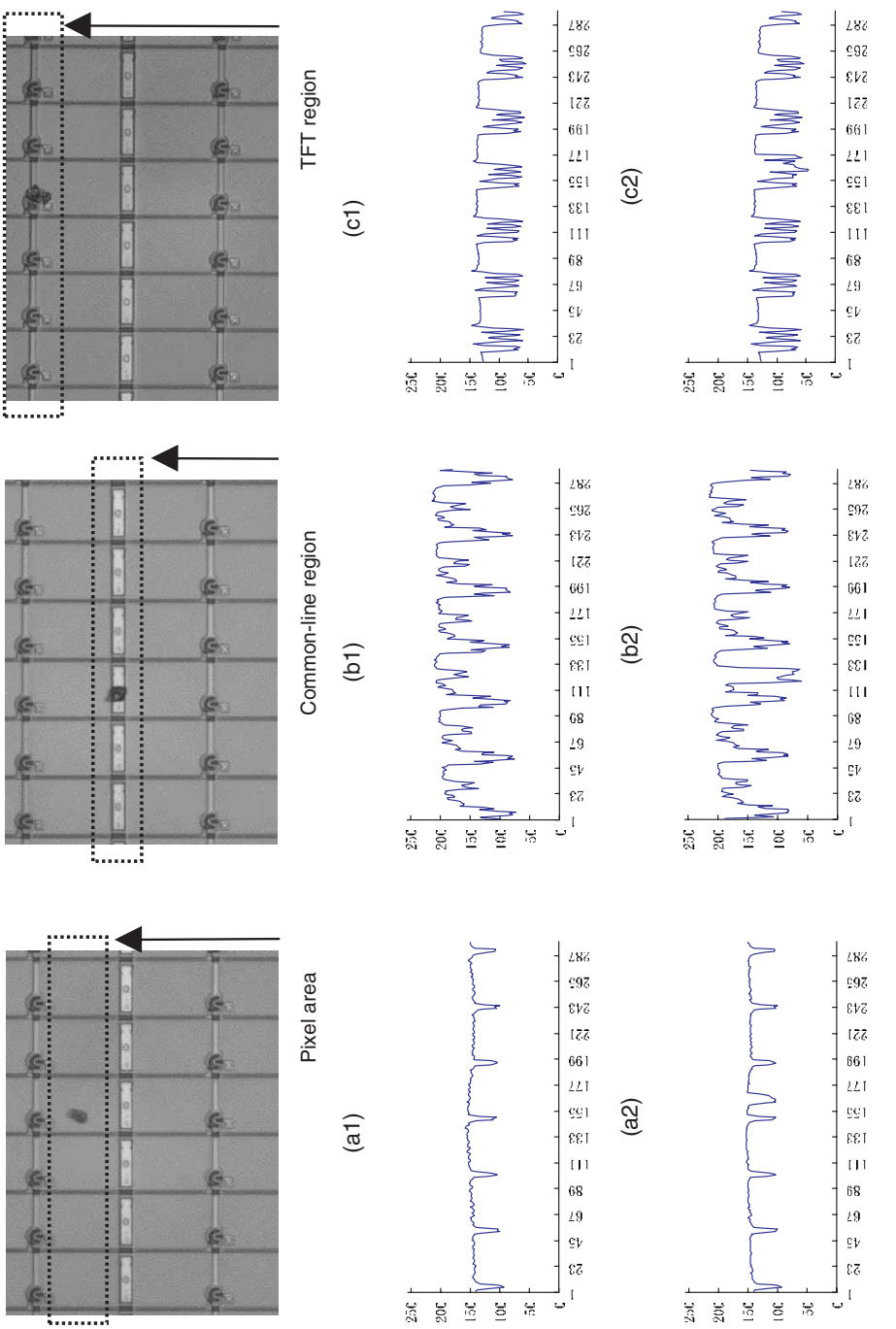

Figure 3. One-dimensional grey level profiles in different TFT-LCD surface regions: (a1–c1) two-dimensional TFT-LCD panel images with a particle defect in the pixel area, common-line region and TFT region, respectively; (a2–c2) respective one-dimensional grey-level profiles in faultless regions; (a3–c3) respective one-dimensional grey-level profiles in defective regions.

Let $f_y(x)$ be the grey level at pixel location x of a line image y, and N be the length of the line image. The 1D discrete Fourier transform of $f_y(x)$ is given by:

$$F_y(u) = \frac{1}{N}\sum_{x=0}^{N-1} f_y(x) \cdot \exp[-j2\pi ux/N] \tag{1}$$

for frequency variable $u = 0, 1, 2, \ldots, N-1$. The Fourier transform is generally complex:

$$F_y(u) = R_y(u) + j \cdot I_y(u),$$

where $R_y(u)$ and $I_y(u)$ are the real and imaginary parts of $F_y(u)$, i.e.:

$$R_y(u) = \frac{1}{N}\sum_{x=0}^{N-1} f_y(x) \cdot \cos(2\pi ux/N) \tag{2}$$

$$I_y(u) = \frac{1}{N}\sum_{x=0}^{N-1} f_y(x) \cdot \sin(2\pi ux/N) \tag{3}$$

The power spectrum $P_y(u)$ of $F_y(u)$ is given by:

$$P_y(u) = R_y^2(u) + I_y^2(u) \tag{4}$$

The 1D inverse Fourier transform is defined by:

$$f_y(x) = \sum_{u=0}^{N-1} F_y(u) \cdot \exp[\, j2\pi ux/N] \tag{5}$$

Figures 4(a1) and (a2) show, respectively, a faultless grey-level profile and its corresponding Fourier spectrum of a TFT-LCD at a coarse resolution of 60 pixels/mm, as that shown in figure 1(a). Tsai and Hung (2005) showed that the relationship between the distance Δx of two adjacent data lines in the grey-level profile and the spacing Δu of two neighbouring peaks in the corresponding Fourier spectrum is given by:

$$\Delta u = \frac{N}{\Delta x}. \tag{6}$$

Therefore, the periodic peaks that represent the data lines in the 1D spatial domain image can be effectively removed by setting the frequency components in the vicinity of every local peak in the Fourier spectrum to zero, and then back-transforming to the spatial-domain image using the 1D inverse Fourier transform in equation (5). Figure 4(a3) demonstrates that the reconstructed 1D image is uniformly flat, and the background pattern of data lines is effectively removed. Figure 4(b1) presents a grey-level profile that crossovers a particle defect in the coarse resolution TFT-LCD panel image. Figure 4(b2) is the corresponding Fourier spectrum. It can be observed from figure 4(b3) that the reconstructed 1D line image distinctly preserves the local anomaly, while the background pattern of periodic peaks are well removed.

In this study, the MVA TFT-LCD panel images at a high resolution contain various complicated patterns other than simple periodic peaks. A TFT-LCD grey-level profile at a low-resolution image can be considered as a well-stationary

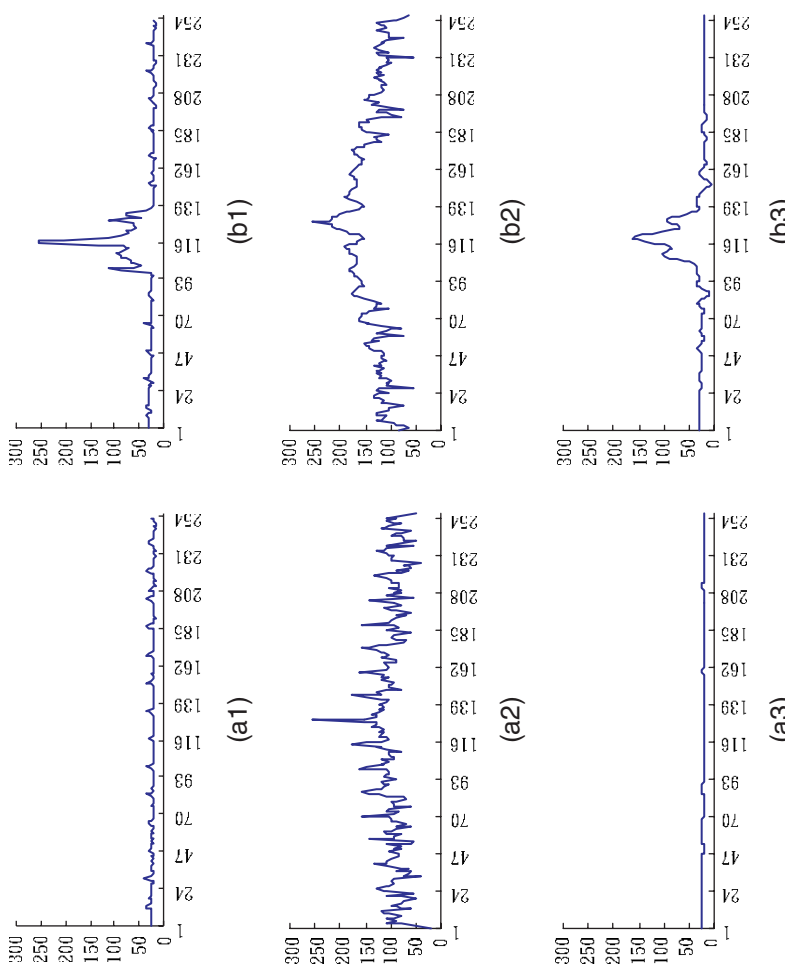

Figure 4. (a1) Faultless line image of a TN TFT-LCD panel at a low resolution of 60 pixels/mm; (b1) defective line image at the same low resolution; (a2) and (b2), respective Fourier power spectra of (a1) and (b1); (a3) and (b3), respective Fourier reconstructed images of (a1) and (b1).

signal with high regularity, while the one at a high-resolution image is a less-stationary signal. Therefore, the 1D Fourier spectrum of such a signal at a high-resolution image is much more difficult to analyse. The proposed 1D image reconstruction scheme of Tsai and Hung (2005) fails to detect micro-defects in a high-resolution TFT-LCD panel image. Figure 5(a1) illustrates a grey-level profile crossing over the common-line region (figure 3(b1)). Since the periodic pattern is much more complicated than the one with simple periodic peaks, the corresponding Fourier spectrum in figure 5(a2) also becomes difficult to analyse. The relationship defined in equation (6) cannot be used sufficiently to remove the background pattern. Figure 5(b1) is a defective version of the grey-level profile that crossovers a defective common-line region. Figures 5(b2) is the corresponding Fourier spectrum. Figures 5(a3) and (b3) are the respective reconstructed line images of figures 5(a1) and (b1) using the 1D reconstruction scheme proposed by Tsai and Hung (2005). The local anomaly cannot be reliably identified from the reconstructed line image.

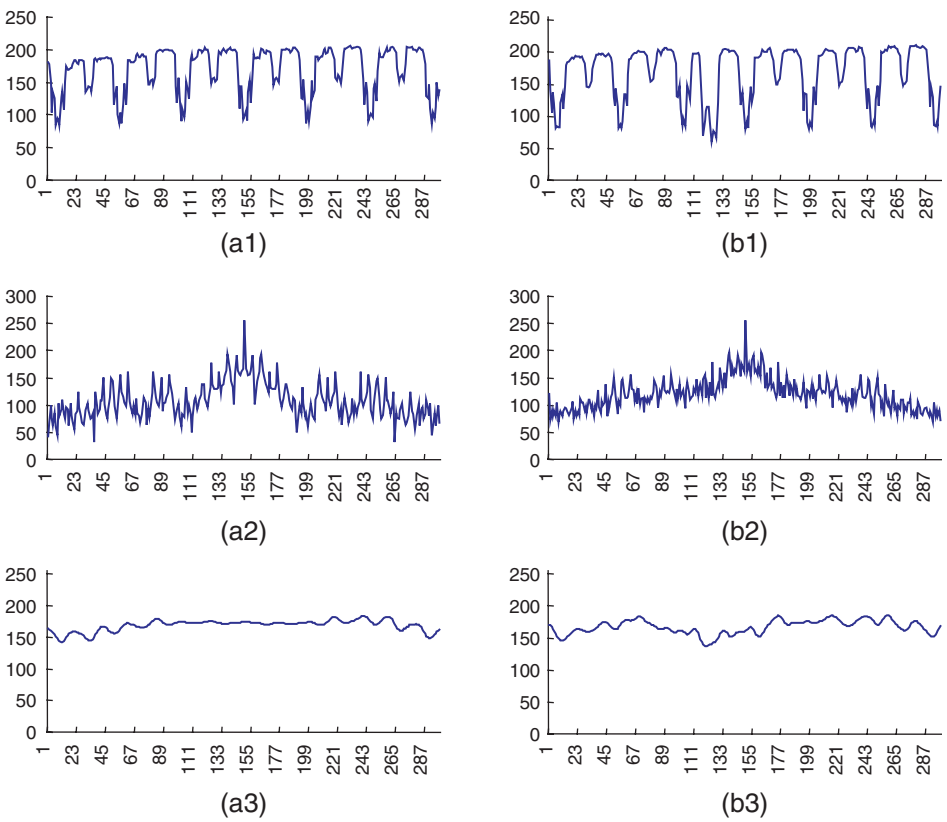

Figure 5. (a1) Faultless line image of an MVA TFT-LCD panel at a high resolution of 500 pixels/mm; (b1) defective line image at the same high resolution; (a2) and (b2), respective Fourier power spectra of (a1) and (b1); (a3–b3) respective Fourier reconstructed images of (a1) and (b1) using the algorithm of Tsai and Hung (2005).

Since the frequency components associated with the global, repetitive background pattern of a TFT-LCD line image at a high resolution cannot be effectively extracted in the 1D Fourier spectrum, the 1D grey-level profile is divided into small segments of equal length and recombined as a 2D image so that the background pattern can be easily recognized in the corresponding 2D Fourier spectrum. As mentioned in section 2.1, any scan lines of the TFT-LCD panel surface have the same period defined by the distance between two neighbouring data lines. Let P be the known spacing in pixel between two adjacent data lines. P is then the period of a 1D line image for the TFT-LCD panel image at a given resolution.

To construct a 1D grey-level profile into a 2D image, each scan line $f_y(x)$ is divided into small segments, each of equal length P, i.e:

$$\begin{aligned} \boldsymbol{s}_{y_i} &= \left\{\hat{f}_{y_i}(k); \quad k = 0, 1, 2, \ldots, P-1\right\} \\ &= \left\{f_y(i \cdot P + k); \; k = 0, 1, 2, \ldots, P-1\right\}, \quad \text{for } i = 0, 1, 2, \ldots, [N/P] - 1 \end{aligned} \tag{7}$$

where $\boldsymbol{s}_{yi}$ is the i-th segment of a scan line y; $\hat{f}_{y_i}(k)$ is the grey level of the k-th pixel in segment $\boldsymbol{s}_{yi}$, which is given by $f_y(i \cdot P + k)$.

Figure 6 depicts the partition of a scanned line image into small segments of length P from left to right. The right-most segment in the resulting partition may not result in a full length of a period P. It is thus discarded in the combination of a 2D image. To inspect defects in such a segment, we may have to redo the partition from right to left so that the right-most segment is of a full period. The divided segments of a 1D scan line $\hat{f}_{y_i}(k)$ are combined as a 2D image $f_y(i, k)$ by:

$$f_y(i, k) = \hat{f}_{y_i}(k), \qquad i = 0, 1, 2, \ldots, [N/P] - 1; \quad k = 0, 1, 2, \ldots, P-1.$$

The number of the divided segments is $[N/P]$, each segment of the length P. Therefore, the combined 2D image is of the size $[N/P] \times P$.

The micro-defects in a TFT-LCD panel image generally have low intensities, and the corresponding grey values $f_y(x)$ are small. To enhance their significance in the Fourier spectrum, the complement of $f_y(x)$ is applied first, i.e.:

$$f_y(x) = 255 - f_y(x)$$

for an 8-bit display system. Figures 7(a1) and (b1) show, respectively, a faultless grey-level profile and a defective version of the profile crossing over the common-line region. The defective scanned line is obtained from the test image shown in figure 8. Figures 7(a2) and (b2) are the corresponding combined 2D images; figures 7(a3) and (b3) show the combined 2D images row by row (i.e. segment by segment) in detail.

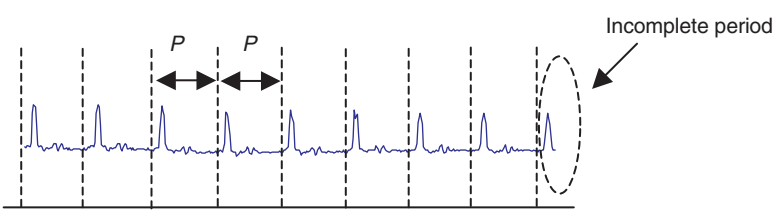

Figure 6. Partition of a line image into small segments of equal length P from left to right.

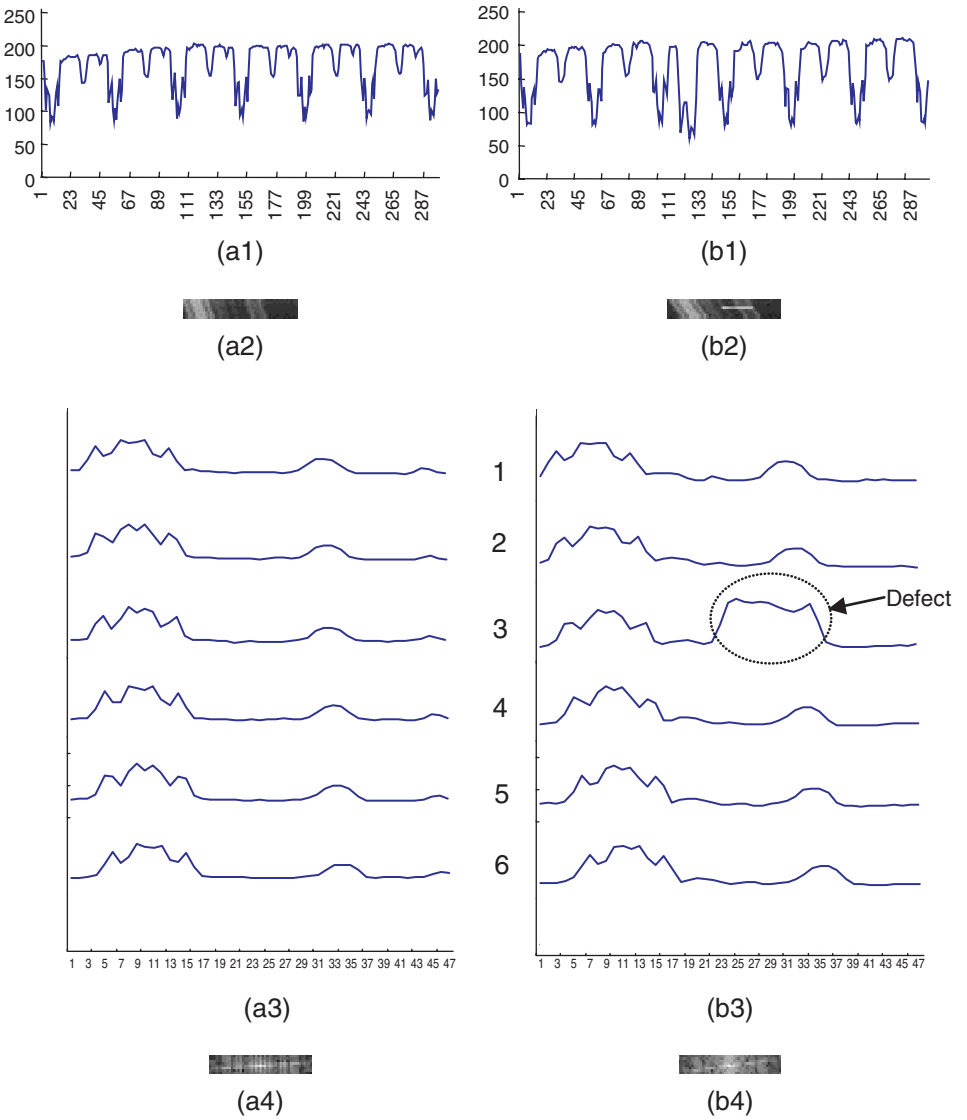

Figure 7. (a1) Faultless line image across the common line, (b1) defective line image across a particle on the common line; (a2) and (b2), respective combined two-dimensional images from one-dimensional divided segments; (a3) and (b3), row-by-row complemented grey levels in the respective combined two-dimensional images; (a4–b4) respective two-dimensional Fourier power spectra of (a2) and (b2).

It can be observed from the figures that the repetitive pattern in a 1D scan line results in an oriented line structure in the combined 2D image. The periodically occurring features of structural lines, therefore, can be easily identified from the magnitude of frequency components in the 2D Fourier-domain image. The directional characters of a spatial-domain grey level image clearly correspond to high-energy frequency components which distribute along the lines in the Fourier-domain image with the

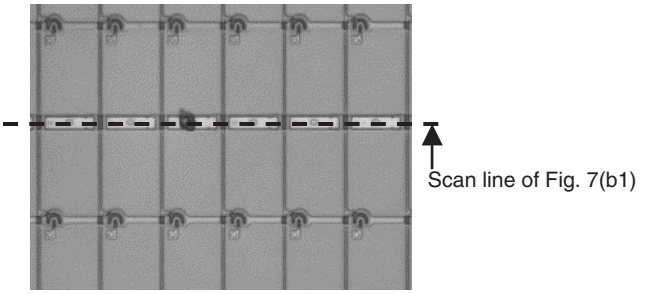

Figure 8. Defective MVA TFT-LCD panel image containing a particle blemish on the common line.

directions orthogonal to their counterparts in the spatial-domain image (Gonzalez and Woods 2002). The transform of repetitive vertical lines in the spatial-domain image appears a horizontal line passing through the centre in the Fourier-domain image. Deleting the repetitive structural lines in the combined 2D image is, therefore, equivalent to the removal of the repetitive background pattern in the original 1D grey-level line image.

The discrete two-dimensional Fourier transform of the combined 2D image $f_y(i,k)$ is given by

$$F_y(u,v) = \frac{1}{[N/P]\cdot P}\sum_{i=0}^{[N/P]-1}\sum_{k=0}^{P-1} f_y(i,k)\exp\left[-j2\pi\left(\frac{ui}{[N/P]}+\frac{vk}{P}\right)\right], \tag{8}$$

where $u=0,\ 1,\ 2,\ldots,[N/P]-1$ and $v=0,\ 1,\ 2,\ldots,P-1$. The power spectrum $P_y(u,v)$ of $F_y(u,v)$ is defined the same as in equation (4). Figures 7(a4) and (b4) present the 2D Fourier spectra of the combined 2D images in figures 7(a2) and (b2), respectively.

Since the oriented line structures appearing in the combined 2D image are approximately vertical, the corresponding frequency components with high power magnitudes are closely distributed along a horizontal line in the Fourier-domain image. The local anomaly in the spatial-domain image contributes significant power magnitudes around the centre of the Fourier-domain image. Given the Fourier spectrum of any grey-level image, the frequency components around the centre of the Fourier plane are low-frequency bands that represent the coarse approximation of the original grey-level image or indicate a unique local feature in the spatial-domain image. The frequency components apart from the centre of the Fourier plane are high-frequency bands that represent the global details of the original grey-level image.

Since the periodic pattern in a 1D scan line results in an oriented line structure in the combined 2D image, the frequency components in the vicinity of the horizontal line and the vertical line passing through the centre of the Fourier plane are set to zero so that the repetitive background pattern in the original 1D scan line can be removed in the reconstructed image using the 2D inverse Fourier transform. In order to smooth further the residuals in the Fourier-reconstructed image, the frequency components in the high-frequency bands are also set to zero so that the global details

of the original signal will not appear in the reconstructed image. The Fourier spectrum is symmetric to the centre of the Fourier plane for a real function $f_y(i,k)$. Every transformed line in the Fourier-domain image will pass through the centre of the Fourier plane.

Let w be the notch width that determines the neighbourhood region for the frequency components along both the horizontal line and vertical line passing through the centre of the Fourier plane. The width w is used to compensate the orientation deviation from the exact vertical direction for the resulting line structure in the combined 2D image. The width w is an odd number and is expressed as $w = 2 \cdot \Delta w + 1$ for some non-negative integer Δw. Also, let r be the parameter that determines the region of the high-frequency band. Figure 9 shows the notation of notch width w and high-frequency region r. All frequency components within the horizontal and vertical notches defined by w with $w = 2 \cdot \Delta w + 1$ and the high-frequency band defined by r are set to zero, i.e.:

$$F_y(u,v) = 0, \quad \text{for all } v, \text{ and } [N/2P] - \Delta w \le u \le [N/2P] + \Delta w \tag{9a}$$

$$F_y(u,v) = 0, \quad \text{for all } u, \text{ and } [P/2] - \Delta w \le v \le [P/2] + \Delta w \tag{9b}$$

$$F_y(u,v) = 0, \quad \text{for all } u, \text{ and, } v \le r \text{ or } v \ge r\ P - r - 1 \tag{9c}$$

Note that the centre of the Fourier plane is at coordinates $([N/2P],[P/2])$ for the combined 2D image of size $[N/P] \times P$. With the newly assigned values of $F_y(u,v)$, the combined 2D image can be reconstructed using the following 2D inverse Fourier transform:

$$\hat{f}_y(i,k) = \sum_{u=0}^{[N/P]-1} \sum_{v=0}^{P-1} F_y(u,v) \exp\left[j2\pi \left(\frac{ui}{[N/P]} + \frac{vk}{P} \right) \right]. \tag{10}$$

Once the 2D Fourier-reconstructed image is obtained, it is converted back to the 1D line image by:

$$\hat{f}_y(i \cdot P + k) = \hat{f}_y(i,k), \quad \text{for } i = 1, 2, \ldots, [N/P] - 2, \tag{11}$$

where $k = 0, 1, 2, \ldots, P-1$.

Figures 10(a1) and (a2) show, respectively, the reconstructed results of the faultless line image in figure 7(a1) from $w = 1$ and 3 with $r = 0$ (i.e. all high-frequency components are retained in the reconstruction). Figures 10(b1) and (b2) show the same reconstruction operations for the defective line image in figure 7(b1).

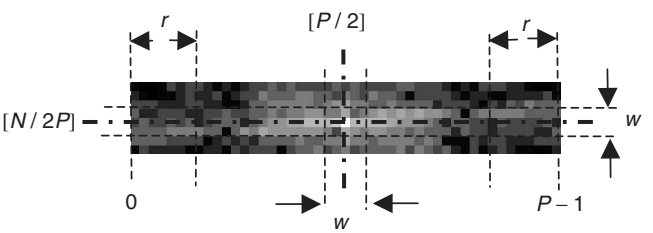

Figure 9. Parameters w and r that define the notch width and high frequency regions, respectively, in the two-dimensional Fourier-domain image of size $[N/P] \times P$.

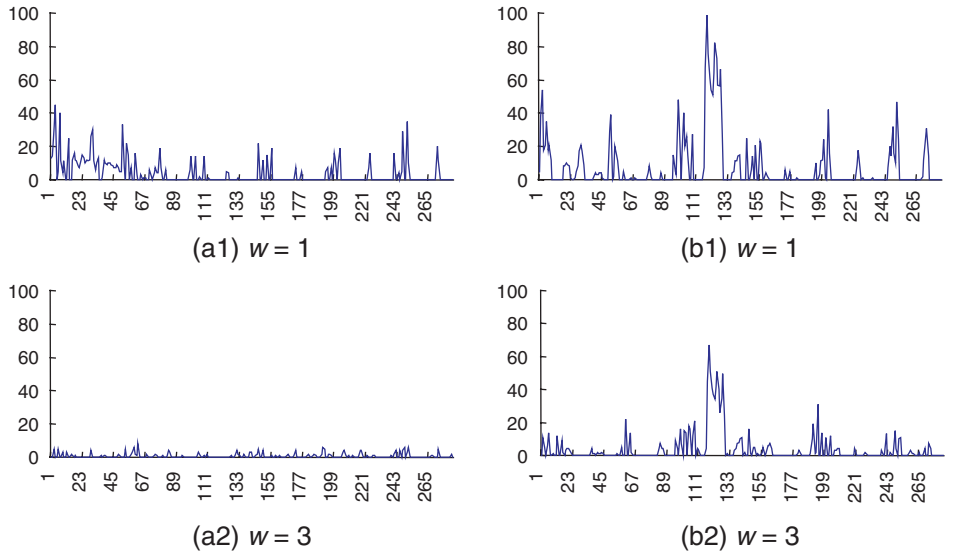

Figure 10. (a1) and (a2), reconstructed line images of the faultless line image in figure 7(a1) with $w = 1$ and 3, respectively; (b1) and (b2), respective reconstructed line images of the defective line image in figure 7(b1) with $w = 1$ and 3 ($r = 0$ is applied for both test line images).

The reconstruction results in figure 10 reveal that the repetitive background pattern of the grey-level profile cannot be completely removed with $w = 1$. The background pattern is well removed and the local anomaly is distinctly preserved with $w = 3$, although some residual details are still retained in the reconstruction.

Figures 11(a1–a4 and b1–b4) demonstrate further the reconstruction results of the faultless line image in figure 7(a1) and the defective line image in figure 7(b1) from varying high-frequency region $r = 10$, 15, 20 and 22 with a fixed notch width $w = 3$. It is apparent from the reconstruction results in figure 11 that an overly small r cannot sufficiently remove residual details, while an excessively large r will oversmooth both the background pattern and the local anomaly. When $r = 15$ or 20, all background patterns are effectively removed in both faultless and defective line images, while a high fluctuation of grey levels associated with the defect is very well preserved. For the given image resolution of 500 pixels/mm, the width parameter $w = 3$ and the high-frequency region parameter $r = 15$ generally give the best reconstruction results for inspection of micro-defects in patterned TFT-LCD panel surfaces. Figures 12 and 13 demonstrate further the reconstruction results of 1D grey-level profiles crossing over the pixel area and the TFT region, respectively, with $w = 3$ and $r = 15$. The results show that subtle defects can be reliably identified for both the highly regular grey-level profile in figure 12(b1) and the less-stationary grey level profile in figure 13(b1).

In addition to the combinations of parameter values $w = 3$ and $r = 10$, 15, 20 and 22, we also examined the reconstruction results from the parameter setting of $w = 1$ and $r = 10$, 15, 20 and 22. The results showed that the reconstructed profiles are better smoothed compared with the ones shown in figures 10(a1) and (b1) with $w = 1$ and $r = 0$. However, the periodic pattern of a faultless scan line still cannot be

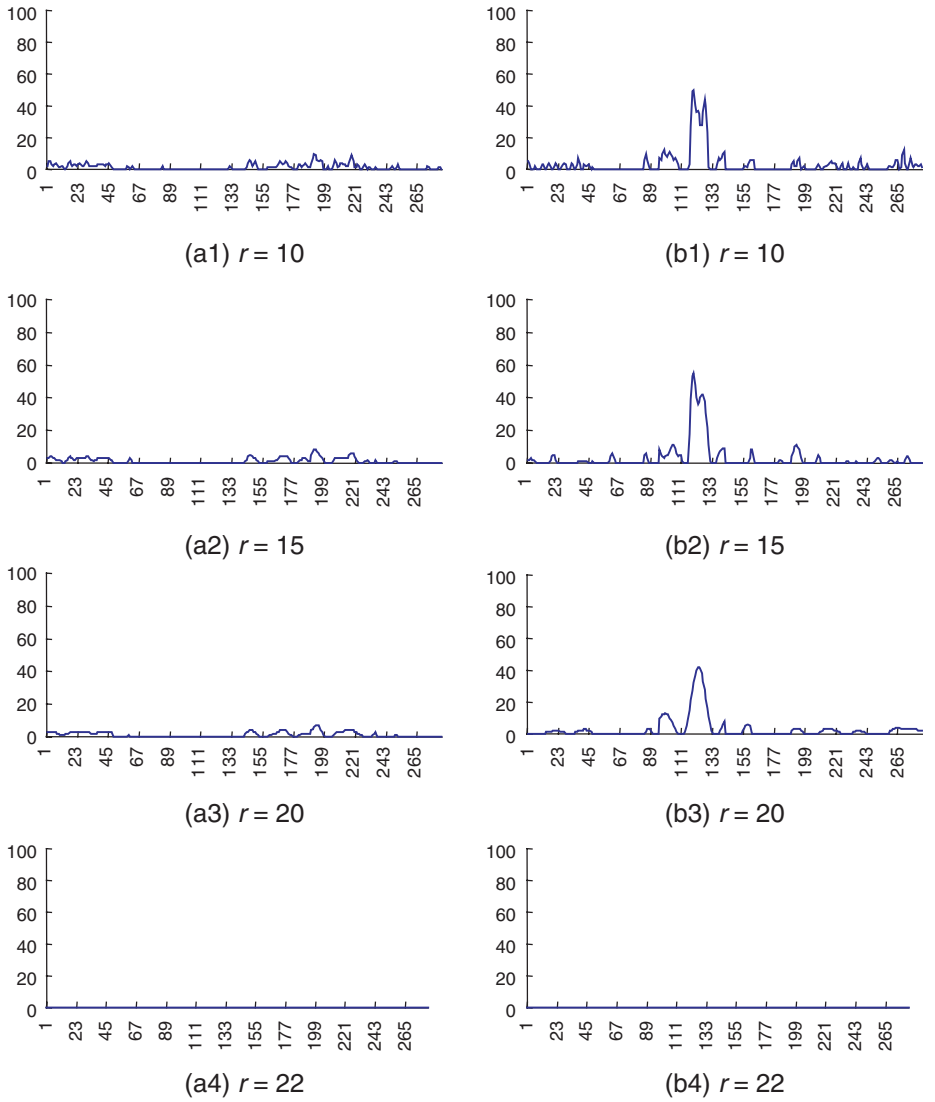

Figure 11. (a1–a4) Reconstructed line images of the faultless line image in figure 7(a1) with $r = 10$, 15, 20 and 22, respectively; (b1–b4) respective reconstructed images of the defective line image in figure 7(b1) with $r = 10$, 15, 20 and 22 ($w = 3$ is applied for the two test line images).

effectively removed. Since the number of the divided segments is generally small with respect to the length of the period in a scan line, a small width value of $w = 3$ is generally sufficient for removing line patterns in the combined 2D image. The frequency components in the high-frequency band represent the details of the original spatial image. Therefore, a larger high-frequency region r may be required for a more complicated pattern of TFT-LCDs.

All the test images demonstrated above show that the reconstructed line image is approximately uniform for a faultless grey-level profile, while the variation in the

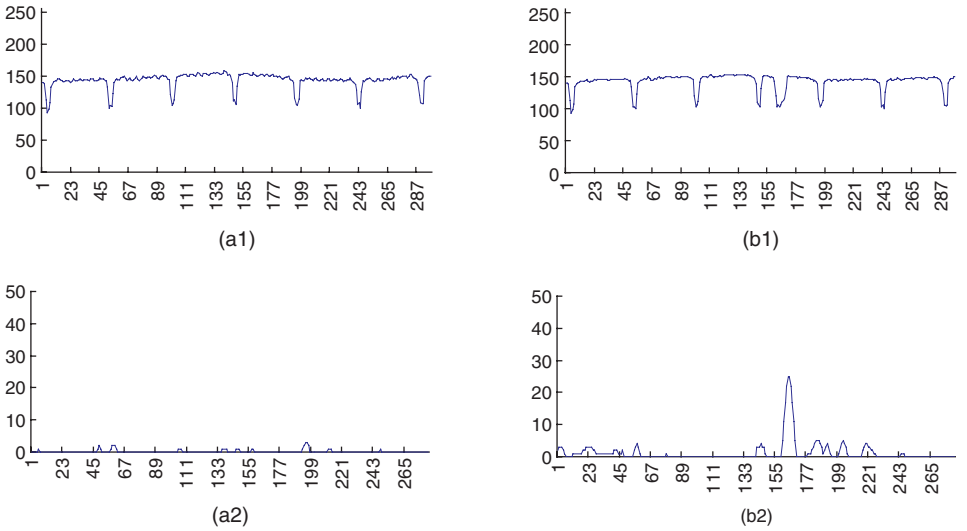

Figure 12. (a1) and (b1) Faultless and defective line images across the pixel area of a TFT-LCD panel; (a2) and (b2), respective reconstructed line images of (a1) and (b1) with $w = 3$ and $r = 15$.

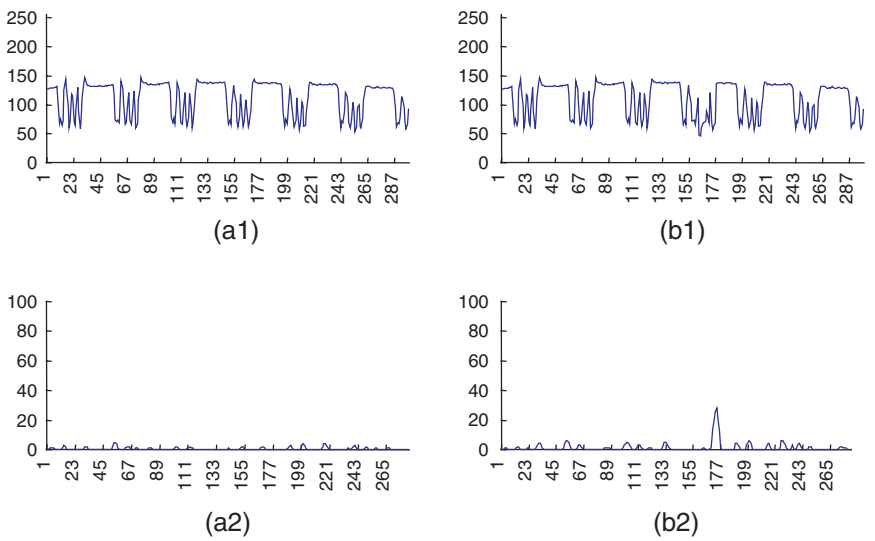

Figure 13. (a1) and (b1) Faultless and defective line images across the TFT region of a TFT-LCD panel; (a2) and (b2), respective reconstructed line images of (a1) and (b1) with $w = 3$ and $r = 15$.

reconstructed line image is significantly high for a defective grey-level profile. Therefore, a simple dual thresholding based on the statistical process control limits can be used to distinguish the anomalies from the uniform background in the reconstructed image. The upper and lower control limits for grey-level variation

in each individual reconstructed 1D image $\hat{f}_y(x)$ are given by:

$$\mu_{\hat{f}_y} \pm K \cdot \sigma_{\hat{f}_y}, \tag{12}$$

where $\mu_{\hat{f}_y}$ and $\sigma_{\hat{f}_y}$ are the mean and standard deviation of grey levels in the whole reconstructed 1D image. Since the grey levels of an anomaly are distinctly different from those of the uniform background in the reconstructed 1D image, the control constant K in equation (12) is set to 4 in this study.

3. Experimental results

This section presents experimental results from a number of micro-defects embedded in different regions of TFT, common-line and pixel area of TFT-LCD panels to evaluate the efficacy of the proposed defect detection scheme. The experiments were conducted on a Pentium IV, 2.4-GHz computer. To visualize the detection results, the test images were displayed in two dimensions of size 223×298 pixels. That is, a 2D test image comprises 223 scan lines, each of the length 298 pixels. All test images were taken at a high resolution of 500 pixels/mm with 8-bit grey levels. Under such a resolution, the period of all TFT-LCD line images for inspection is 47 pixels. The two parameters of the notch width and the high-frequency region used for the Fourier reconstruction were given by $w = 3$ and $r = 15$ (see equation 9) for all test images in the experiments. The control constant $K = 4$ (see equation 12) was used to set up the control limits for all test images. Points falling within and outside the control limits are respectively represented by white and black intensities so that the detected defects can be easily observed and verified in the binarized image.

Figures 14(a1–c1) show, respectively, three defective 2D images containing particle blemishes in pixel area, common-line region, and TFT region of TFT-LCD panel surfaces at the resolution 500 pixels/mm. Figure 14(d1) illustrates a faultless 2D image of the TFT-LCD panel at the same resolution. The micro-defects must be detected in images at such a fine resolution. They become blurred or invisible at lower resolutions. Figures 14(a2–d2) present the detection results of the four test images in figures 14(a1–d1), respectively. Each 2D binary image in figures 14(a2–d2) is the result of merging all the 223 filtered line images in their scanning sequence. In the defective images of figures 14(a1–c1), the particle defects are well detected and located, regardless of their positions in the TFT-LCD panel surface. Note that the hardly visible particle embedded in the complicated TFT region is also reliably detected, as shown in figures 14(c1) and (c2). For the faultless TFT-LCD surface image of figure 14(d1), the resulting 2D binary image in figure 14(d2) is uniformly white, except for a few noisy points of size 1 or 2 pixels.

Figures 15(a1–c1) present further three defective TFT-LCD images containing a water stain, a long fibre, and a tiny fibre falling on the data line, respectively. The detection results shown as binary images in figures 15(a2–c2) indicate that the proposed 1D image reconstruction scheme can well detect the locations and shapes of local faulty items. The short fibre that vertically falls on one of the vertical data lines is also reliably detected, as shown in figure 15(c2).

To demonstrate further the robustness of the proposed method under varying illumination, figures 16(a–f) show, respectively, six versions of a defective image

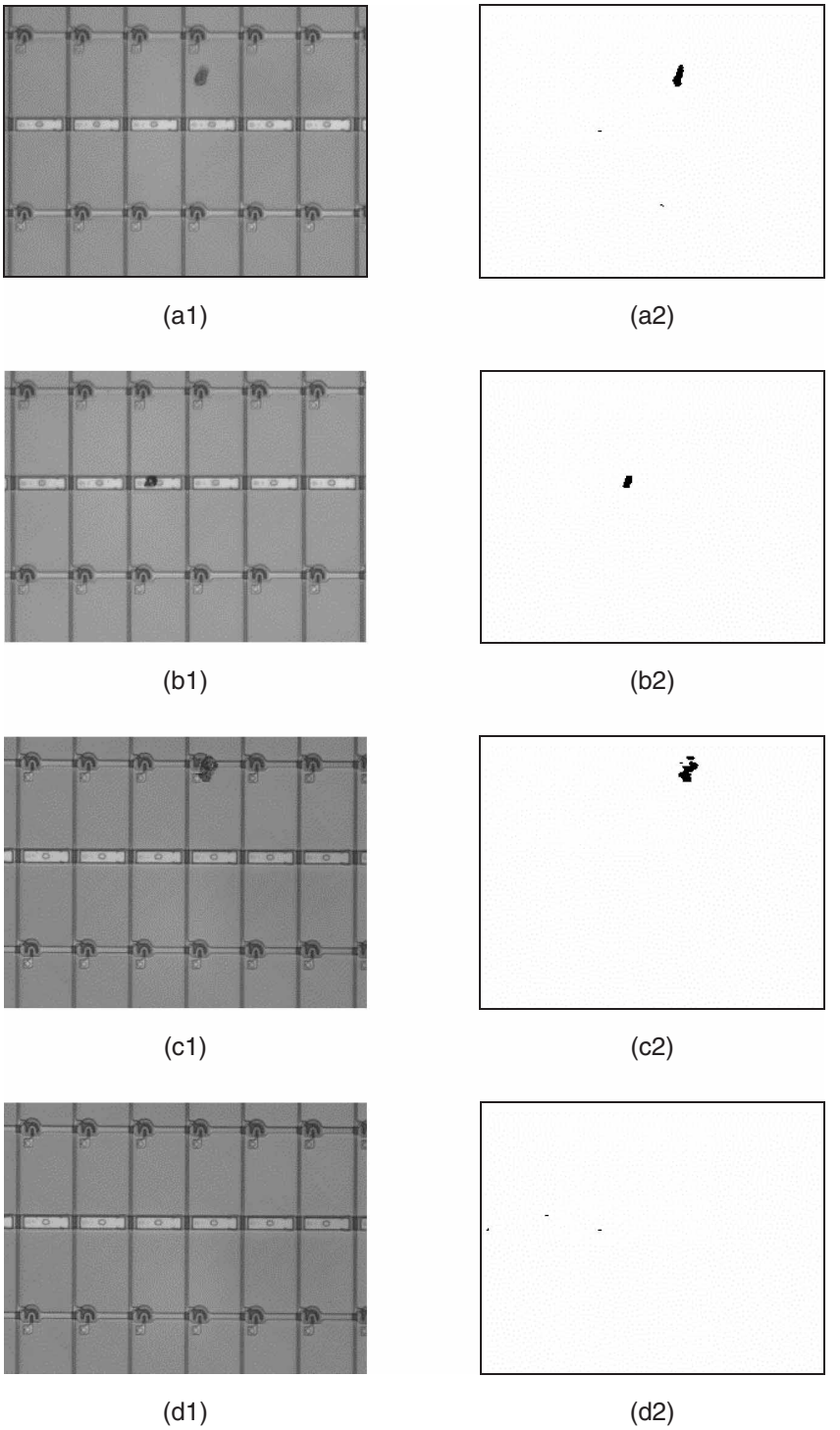

Figure 14. (a1–c1) Three defective TFT-LCD panel images with a particle blemish in the pixel area, common-line region and TFT region, respectively; (d1) faultless version of the TFT-LCD panel; (a2–d2) detection results as merged binary images for (a1–d1), respectively.

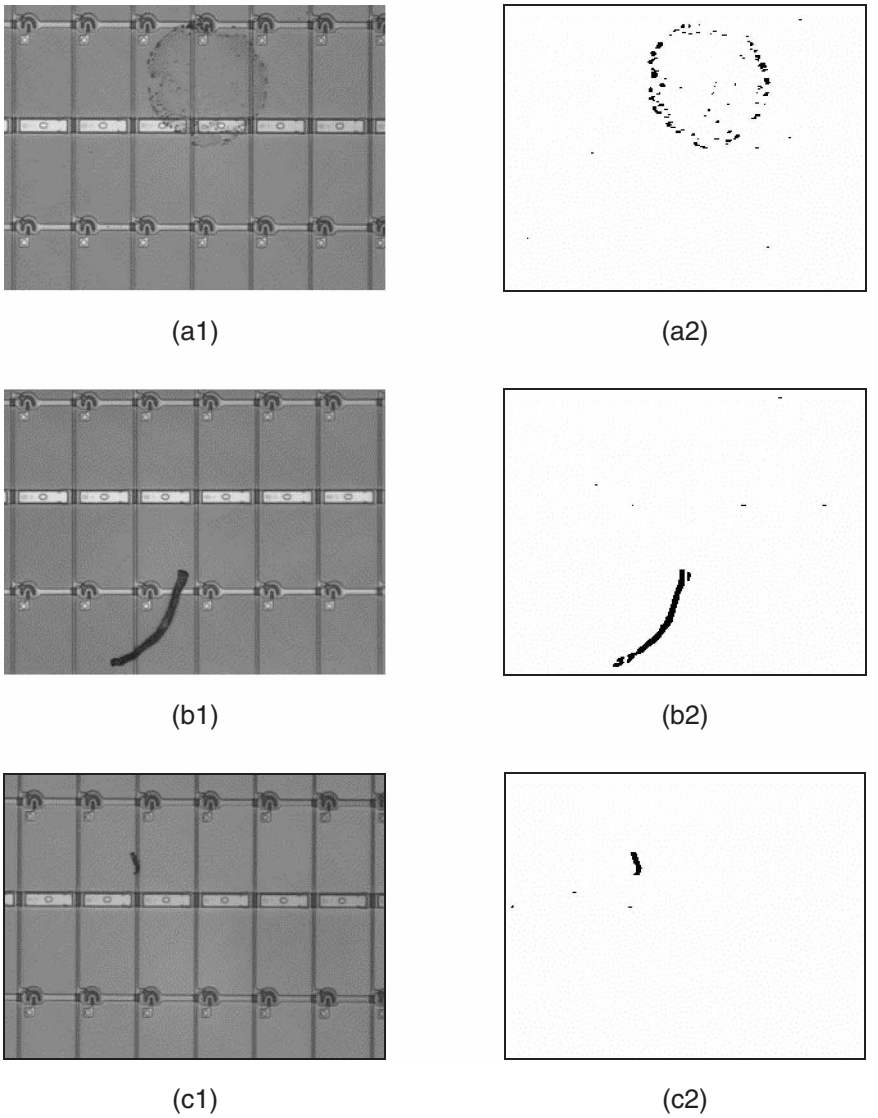

Figure 15. (a1) Defective TFT-LCD image containing a water stain; (b1) defective image containing a long fibre; (c1) defective image containing a tiny fibre falling on the data line; (a2–c2) respective detection results as merged binary images for (a1–c1).

(a particle in the pixel area) under illumination levels of 250, 500, 750, 1000, 1250 and 1500 lux, of which 750 lux is the original set-up of lighting. Note that figures 16(a) and (f) are two highly under- and overexposed images for inspection. The detection results shown as merged 2D binary images are presented in figures 17(a–f). They show that the particle blemish is reliably detected for the test images under the illumination between 750 and 1500 lux. The defect can also be detected in the excessively dark images of figures 16(a) and (b), except that some residual points

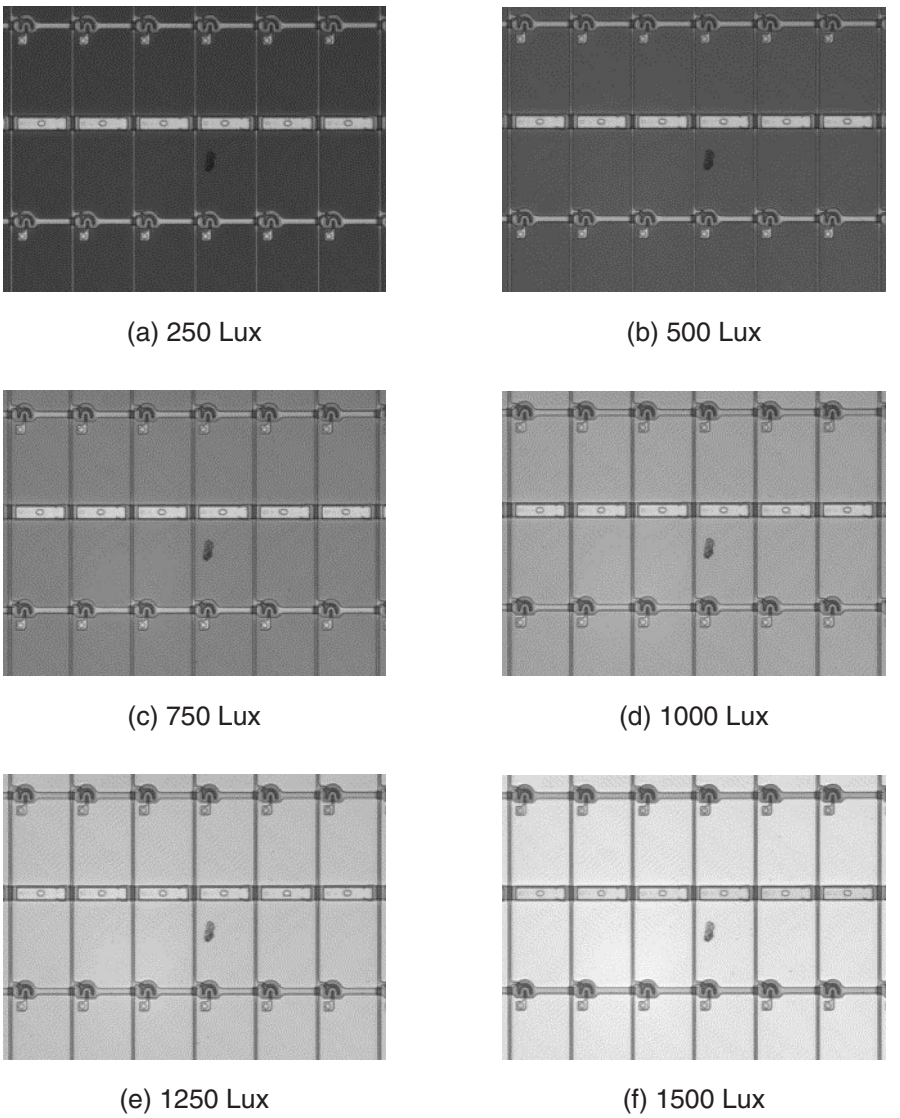

Figure 16. (a–f) Defective TFT-LCD panel image under varying illumination levels of 250, 500, 750, 1000, 1250 and 1500 lux, respectively.

of the background pattern are also presented. The experiments on the effect of varying illumination reveal that the proposed method is not sensitive to changes in illumination. A sufficient illumination is always recommended in the inspection process for better detection with minimum noisy points.

The proposed Fourier reconstruction scheme is invariant to horizontal and vertical translations since the inspection is based on individual line images. Actually, the test sample images in figures 14(a1–d1) and 15(a1–c1) can be considered as different translation versions of a TFT-LCD panel surface because their topmost

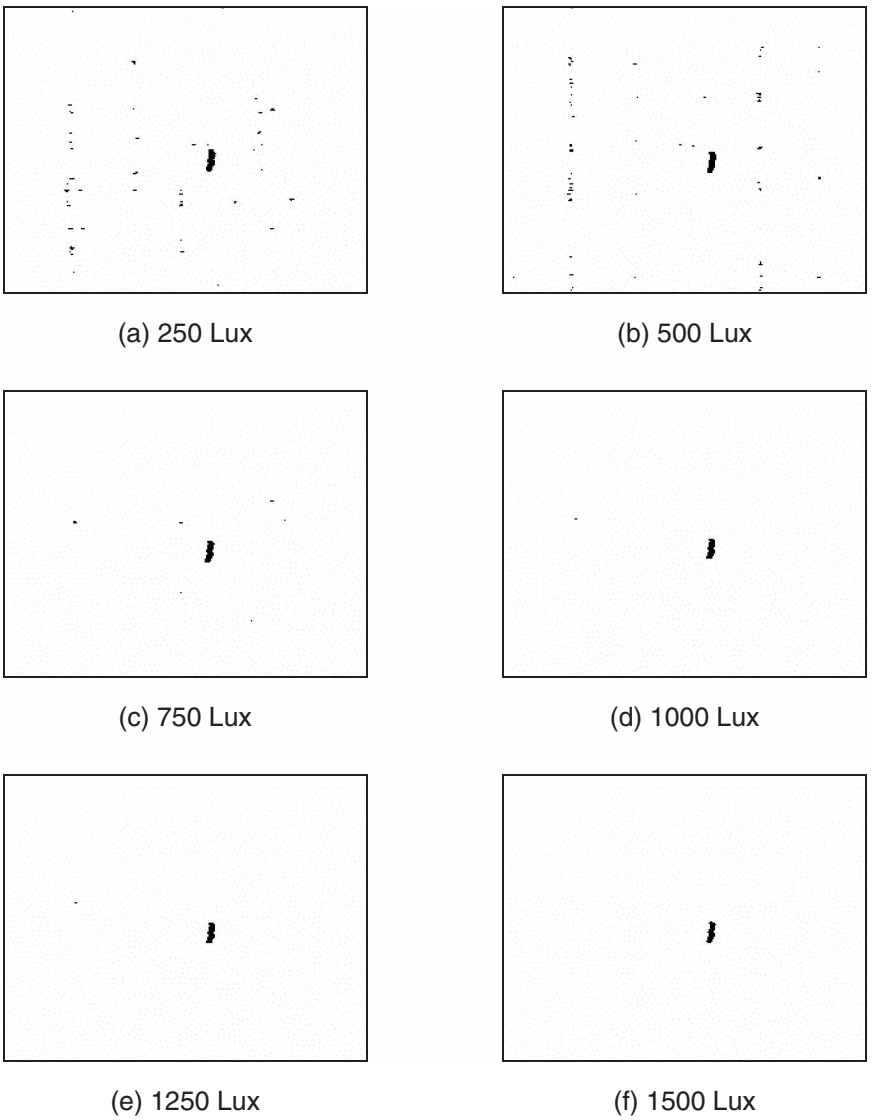

Figure 17. (a–f) Detection results as merged two-dimensional images for the test images in figures 16(a–f), respectively.

horizontal rows and the left-most vertical columns are quite different. The test images in figures 14(d1) and 15(c1) even show a few degrees of rotation. However, the proposed method is rotation-dependent. In practical implementation, the inspection panel in an LCD manufacturing process can be well positioned, especially in angular orientation, by a mechanical alignment system. To ensure further the correct orientation of an inspection panel, one can obtain a small 2D image of the panel surface before the inspection process proceeds. Since the panel surface basically comprises vertical data lines and horizontal gate lines in the image,

the orientation of the dominant line pattern in the 2D spatial domain image can be determined easily by detecting the high-energy frequency components in the corresponding 2D Fourier domain image using a 1D Hough transform, as proposed by Tsai and Hsieh (1999). The orientation of the inspection panel can then be adjusted so that the data lines become strictly vertical in individual scan line images.

4. Conclusions

The traditional pattern-matching technique has been a commonly used machine vision method in industry inspection applications. It is straightforward and computationally fast. However, it requires a large storage volume of data for the reference template, and precise environmental controls such as lighting and alignment of image translation. The present paper has presented a 1D Fourier image reconstruction scheme for automatic visual inspection of micro-defects in TFT-LCD panel surfaces that involve complicated multiple patterns at a high-resolution image. The sensed image for inspection is assumed to be obtained from a line scan system. The proposed method can work directly on 1D line images and, therefore, has the merit in inspecting large-sized TFT-LCD panels that require an extremely high resolution to capture subtle defects of small sizes.

The proposed method does not require the design of quantitative features for various types of defects or a reference template for comparison. It is based on the background-pattern removal strategy using 1D Fourier reconstruction. Since the corresponding 1D Fourier spectrum of a less-regular 1D grey-level profile is difficult to analyse, the original 1D grey-level profile is first divided into small segments, each of equal length of a given period. The divided segments are then combined in their partition sequence as a 2D image. The frequency components associated with the repetitive background pattern can be easily identified as the ones in the neighbourhood of the horizontal line passing through the centre of the 2D Fourier spectrum. By setting such frequency components and those representing the global details of the original image to zero, and then back-transforming the remaining frequency components to the spatial-domain image using the 2D inverse Fourier transform, the repetitive background pattern in a 1D grey-level profile can be effectively removed. A faultless line image of the TFT-LCD panel surface will become an approximately uniform grey-level profile, while anomalies in the defective line image will be distinctly enhanced in the reconstruction.

With the parameter values $w = 3$ (the notch width) and $r = 15$ (the high-frequency region) used for Fourier reconstruction at the given resolution of 500 pixels/mm, experimental results showed that the proposed method is insensitive to illumination changes, and can reliably detect various ill-defined micro-defects embedded in different regions of a TFT-LCD panel surface. The two parameters w and r used for the removal of repetitive background pattern in line images of TFT-LCD panel surfaces may have to readjust for TFT-LCD panels at different image resolutions. This is because that the structural pattern of a TFT-LCD panel at different resolutions may generate distinct repetitive grey-level profiles.

The computation time of the proposed algorithms (including both the Fourier transform and inverse Fourier transform) for a 1024-pixel line image is only 2 ms using the FFTW software library (Frigo and Johnson 2004, 2005) on the Pentium IV

2.4-GHz personal computer. Computation time of the fast Fourier transform can be further improved by implementing the algorithm with a hardware device in the form of Field Programmable Gate Array (FPGA) (Lim and Crosland 2005, Uzun and Bouridane 2005). This should make the proposed Fourier reconstruction scheme practical for defect detection in LCD manufacturing.

Although the anomalies are detected from individual 1D line images in this study, the detection result of the merged 2D binary image shows that the proposed method not only identifies the presence of a local defect, but also locates well the position and preserves the shape of the detected defect. The exact shape of a defect provides important features for the classification of defect types for in-process monitoring and control in LCD manufacturing. Classification of micro-defects in TFT-LCD panel surfaces using the location, intensity, contrast and geometric features of the detected defect is currently under investigation. It is believed that the proposed 1D defect detection scheme can be extended for the inspection of industrial surfaces in general as long as the inspection surface contains a repetitive pattern with a fixed period along every horizontal scan line.

References

Chen, P.O., Chen, S.H. and Su, F.C., An effective method for evaluating the image-sticking effect of TFT-LCDs by interpretative modeling of optical measurement. *Liquid Cryst*., 2000, **27**, 965–975.

Frigo, M. and Johnson, S.G., FFTW web page, 2004. Available online at: http:/www.fftw.org

Frigo, M. and Johnson, S.G., The design and implementation of FFTW3. *Proc. IEEE*, 2005, **93**, 216–231.

Gonzalez, R.C. and Woods, R.E., *Digital Image Processing*, 2002 (Upper Saddle River, NJ: Prentice-Hall).

Hawthorne, J., Electro-optics technology tests flat-panel displays. *Laser Focus World*, 2000, **36**, 271–276.

Henly, F.J. and Addiego, G., In-line functional inspection and repair methodology during LCD panel fabrication, in SID Symposium Digest Paper, 1991, pp. 686–688.

Kido, T., In process functional inspection technique for TFT-LCD arrays. *J. SID*, 1993, **1**, 429–435.

Kido, T., In-processing inspection technique for active-matrix LCD panels, in Proceedings of IEEE International Test Conference, Baltimore, MD, USA, 1992, pp. 795–799.

Kido, T., Kishi, N. and Takahashi, H., Optical charge-sensing method for testing and characterizing thin-film transistor arrays. *IEEE J. Select. Topic. Quant. Elec*., 1995, **1**, 993–1001.

Koike, Y. and Okamoto, K., Super high quality MVA-TFT liquid crystal displays. *Fujitsu Sci. Tech. J*., 1999, **35**, 221–228.

Lim, S.Y. and Crosland, A., Implementing FFT in an FPGA co-processor, 2005. Available online at: http://altera.com/literature/cp/gspx/fft-in-fpga.pdf

Lin, C.S., Wu, W.Z., Lay, T.L. and Chang, M.W., A digital image-based measurement system for an LCD backlight module. *Optic. Laser Tech*., 2001, **33**, 499–505.

Maeda, S., Ono, M., Kubata, H. and Nakatani, M., Precise detection of short-circuit defects on TFT substrate by infrared image matching. *Sys. Comput. Jpn*, 1999, **30**, 72–84.

Nakamura, T., Karube, M., Hayashi, H., Nakamura, K., Tada, N., Fujiwara, H., Tsutsumi, J. and Motai, T., Low temperature poly-Si TFT-LCD with an integrated analog circuit. *J. Soc. Informat. Disp*., 2002, **10**, 203–207.

Nakashima, K., Hybrid inspection system for LCD colour filter panels, in Proceedings of the 10th International Conference on Instrumentation and Measurement Technology, Hamamatsu, Japan, 1994, pp. 689–692.

Nishibe, T., Future for low-temperature polycrystalline silicon, in SID Conference Record of the 22nd International Display Research Conference, Nice, France, October 2002, pp. 269–272.

Oh, J.-H., Kwak, D.-M., Lee, K.-B., Song, Y.-C., Choi, D.-H. and Park, K.-H., Line defect detection in TFT-LCD using directional filter bank and adaptive multilevel thresholding. *Key Eng. Mat.*, 2004, **270–273**, 233–238.

Park, J.H., Choi, Y., Yoon, T.Y., Yu, C.J. and Lee, S.D., A self-aligned multi-domain liquid-crystal display on polymer gratings in a vertically aligned configuration. *J. Soc. Informat. Disp.*, 2003, **11**, 283–287.

Pratt, W.K. and Hawthorne, J.A., Machine vision methods for automatic defect detection in liquid crystal displays. *Adv. Imag.*, 1998, **13**, 52–54.

Sokolov, S.M. and Treskunov, A.S., Automatic vision system for final test of liquid crystal display, in Proceedings of the IEEE International Conference on Robotics and Automation, Nice, France, 1992, pp. 1578–1582.

Tsai, D.M. and Hsieh, C.Y., Automated surface inspection for directional textures. *Image Vis. Comput.*, 1999, **18**, 49–62.

Tsai, D.M. and Hung, C.Y., Automatic defect inspection of patterned thin film transistor-liquid crystal display (TFT-LCD) panels using one-dimensional Fourier reconstruction and wavelet decomposition. *Int. J. Prod. Res.*, 2005, **43**, 4589–4607.

Uzun, I.S. and Bouridane, A.A., FPGA implementations of fast Fourier transforms for real-time signal and image processing, 2005. Available online at: http://www.ce/oxica.com/techlib/files/CEL-W0402101462-250.pdf

Zhang, Y. and Zhang, J., Fuzzy recognition of the defect of TFT-LCD. *Proc. SPIE*, 2005, **5637**, 233–240.